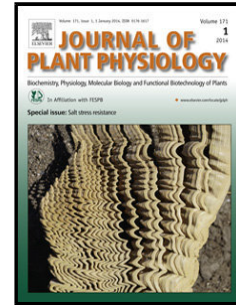


Accepted Manuscript

Title: Microcystin-LR induces mitotic spindle assembly disorders in *Vicia faba* by protein phosphatase inhibition and not reactive oxygen species induction

Author: Tamás Garda Zoltán Kónya Ildikó Tándor Dániel
Beyer Gábor Vasas Ferenc Erdődi György Vereb Georgina
Papp Milán Riba Márta M-Hamvas Csaba Máthé



PII: S0176-1617(16)30048-7
DOI: <http://dx.doi.org/doi:10.1016/j.jplph.2016.04.009>
Reference: JPLPH 52352

To appear in:

Received date: 30-1-2016
Revised date: 4-4-2016
Accepted date: 4-4-2016

Please cite this article as: Garda Tamás, Kónya Zoltán, Tándor Ildikó, Beyer Dániel, Vasas Gábor, Erdődi Ferenc, Vereb Gyddotorgy, Papp Georgina, Riba Milán, M-Hamvas Márta, Máthé Csaba. Microcystin-LR induces mitotic spindle assembly disorders in *Vicia faba* by protein phosphatase inhibition and not reactive oxygen species induction. *Journal of Plant Physiology* <http://dx.doi.org/10.1016/j.jplph.2016.04.009>

This is a PDF file of an unedited manuscript that has been accepted for publication. As a service to our customers we are providing this early version of the manuscript. The manuscript will undergo copyediting, typesetting, and review of the resulting proof before it is published in its final form. Please note that during the production process errors may be discovered which could affect the content, and all legal disclaimers that apply to the journal pertain.

Microcystin-LR induces mitotic spindle assembly disorders in *Vicia faba* by protein phosphatase inhibition and not reactive oxygen species induction

Tamás Garda^{a*}, Zoltán Kónya^{a,b*1}, Ildikó Tándor^a, Dániel Beyer^{a,c2}, Gábor Vasas^a, Ferenc Erdődi^b, György Vereb^d, Georgina Papp^a, Milán Riba^a, Márta M-Hamvas^a, Csaba Máthé^{a**}

^aDepartment of Botany, Faculty of Science and Technology; Departments of ^bMedical Chemistry, ^c Human Genetics, ^d Biophysics and Cell Biology, Faculty of Medicine, University of Debrecen, Egyetem ter 1, H-4032, Debrecen, Hungary

E-mail addresses: gtamas0516@gmail.com; konya.zoltan@med.unideb.hu ;
dike15ster@gmail.com; beyerdani@gmail.com; vasas.gabor@science.unideb.hu;
erdodi@med.unideb.hu; vereb@med.unideb.hu; papp.georgina93@gmail.com;
ribamilan@freemail.hu; hamvas.marta@science.unideb.hu; mathe.csaba@science.unideb.hu

¹present address is ^b

²present address is ^c

* these two authors contributed equally to the present work

**author for correspondence. E-mail: mathe.csaba@science.unideb.hu; Tel.: +36 52 512900;

Fax: +36 52 512943

Abstract

We aimed to reveal the mechanisms of mitotic spindle anomalies induced by microcystin-LR (MCY-LR), a cyanobacterial toxin in *Vicia faba*, a well-known model in plant cell and molecular biology. MCY-LR inhibits type 1 and 2A phosphoserine/threonine specific protein phosphatases (PP1 and PP2A) and induces reactive oxygen species (ROS) formation. The cytoskeleton is one of the main targets of the cyanotoxin during cytopathogenesis.

Histochemical- immunohistochemical and biochemical methods were used. A significant number of MCY-LR induced spindle alterations are described for the first time. Disrupted, multipolar spindles and missing kinetochore fibers were detected both in metaphase and anaphase cells. Additional polar microtubule (MT) bundles, hyperbundling of spindle MTs, monopolar spindles, C- S- shaped, additional and asymmetric spindles were detected in metaphase, while midplane kinetochore fibers were detected in anaphase cells only. Several spindle anomalies induced mitotic disorders, i.e. they occurred concomitantly with altered sister chromatid separation. Alterations were dependent on the MCY-LR dose and exposure time. Under long-term (2 and mainly 6 days') exposure they were detected in the concentration range of 0.1 – 20 $\mu\text{g mL}^{-1}$ MCY-LR that inhibited PP1 and PP2A significantly without significant ROS induction. Elevated peroxidase/catalase activities indicated that MCY-LR treated *V. faba* plants showed efficient defense against oxidative stress. Thus, although the elevation of ROS is known to induce cytoskeletal aberrations in general, this study shows that long-term protein phosphatase inhibition is the primary cause of MCY-LR induced spindle disorders.

Keywords: microcystin-LR, spindle alteration, protein phosphatase, reactive oxygen species, *Vicia faba*

Introduction

Microcystin-LR (MCY-LR) is a cyclic heptapeptide, the most frequently occurring member of a toxin family produced by several freshwater cyanobacterial genera (Campos and Vasconcelos; 2010 Carmichael, 1992). Under certain environmental conditions (high temperature, water eutrophication), overproduction of MCY containing strains, i.e. toxic cyanobacterial blooming occurs, that leads to toxin release into freshwaters - a serious environmental hazard to animal and human health and to aquatic organisms (Codd et al., 2005; Máthé et al., 2007). A wide range of growth, cellular and biochemical effects of MCY-LR have been described in plants (for recent results, see Babica et al., 2006; Chen et al., 2013; Corbel et al., 2014; Máthé et al., 2013a; Žegura et al., 2011). In contrast to inhibitors that predominantly affect a single type of protein phosphatase, MCY-LR binds close to the active centers of type 1 and 2A serine-threonine protein phosphatase (PP1 and PP2A) catalytic subunits (PP1c and PP2Ac) at the hydrophobic substrate binding groove with high affinity and a covalent linkage between the toxin and a Cys residue of PP1c/ PP2Ac forms, resulting in irreversible inhibition of these enzymes. MCY-LR inhibits other Ser/Thr protein phosphatases such as PP4 and PP5 as well (Cohen et al., 2005; MacKintosh and Diplexcito, 2003). In addition, the cyanotoxin is known to induce oxidative stress by increasing ROS levels (probably mainly H₂O₂ and ·OH) both in animals and plants, including organisms that naturally co-exist with toxic cyanobacteria (Campos and Vasconcelos, 2010; Jiang et al., 2011; Pflugmacher, 2002). MCY-LR is known to induce alterations in the cytoskeletal organization of eukaryotic cells, a major cause of toxin-induced histopathology (see; Beyer et al., 2012; Lankoff et al., 2003; Máthé et al., 2009, 2013b; Toivola and Eriksson, 1999 for example). However, cyanotoxin-induced anomalies of mitotic spindle organization in animal

and plant cells are less understood. This topic is important for a better understanding of cellular mechanisms of MCY-LR toxicity.

PP1 and PP2A mediate a significant number of cellular processes in eukaryotes. This includes regulation of the cell cycle and particularly mitotic division (Luan, 2003). In animal and human cells, there is an increasing body of evidence for the active role of PP1 and PP2A in the regulation of G1/S, G2/M transition as well as in the spindle checkpoint (Bollen et al., 2009). However, there is still a need for intensive research concerning the role of protein dephosphorylation in mitotic spindle assembly and functioning- and this is particularly true for plants. This topic is of key importance, since proper organization of spindles- especially their microtubular components - is indispensable for the correct sister chromatid segregation during mitosis (see the review of Kline-Smith and Walczak, 2004). Oxidative stress in general is known to alter microtubule (MT) assembly both in mitotic and non-mitotic animal cells (Wang et al., 2013). MCY-LR-induced ROS elevation influences MT organization, although to date, such evidence exists only for animal/human (mostly non-dividing) cells (see Ding et al., 2001 for an example).

The mitotic apparatus of plant cells bears many similarities to animal cells, but significant differences can be found. With the exception of some cell types, the spindle formed during prophase and prometaphase is anastral. In the absence of centrosomes, the localization and organization of spindle poles and the spindle itself is defined by a peculiar premitotic and early mitotic structure, the preprophase band (PPB). Kinetochore fibers and interpolar MTs are nucleated at multiple microtubule organizing centers (MTOCs) per each pole. Thus, the spindle appears to be composed of less defined, multiple bundles (Ambrose and Cyr, 2008; Baskin, 2000). The regulation of plant spindle formation is a complex process. As for animal cells, the assembly of MT structures is under phosphorylation control at several levels (MAP kinases, cyclin dependent kinases, Aurora kinases) and it is likely to involve

protein phosphatases (Ambrose and Cyr, 2008; Smertenko et al., 2006). Due to the above findings, it is worthwhile to study MCY-LR-affected spindle assembly in all eukaryotic, and particularly, plant cells.

We chose *Vicia faba* (broad bean) for the present study. This plant has proven to be a good model for cell biology and cytogenetical studies in eukaryotes generally and plants in particular (Beyer et al., 2012; Olszewska et al., 1990). The aim of this work was: (i) to reveal all possible types of MCY-LR induced mitotic spindle anomalies in a model plant system as a contribution to the understanding of the mechanisms of its toxicity in dividing eukaryotic cells; and (ii) to answer the question whether protein phosphatase inhibition or ROS induction is the primary cause of MT alterations induced by the cyanotoxin.

1. Materials and methods

1.1. Plant material and MCY-LR treatments

The production of *Vicia faba* (convar. *faba* cv. „Lippói”) axenic seedlings and treatments with purified MCY-LR were performed as described previously (Beyer et al., 2012). The toxin was purified essentially by ion-exchange chromatography and HPLC as described previously (Kós et al., 1995; Vasas et al., 2004). Its purity was $\geq 95\%$. MCY-LR exposure of 5d- pre-germinated seedlings was performed in 100 mL glass vessels, 5 mL MS medium supplemented with Gamborg’s vitamins (Gamborg et al., 1968; Murashige and Skoog, 1962) under a 14/10 h photoperiod and lasted for 1, 2 and 6 days. All experiments (time- and concentration dependent effects of MCY-LR) were repeated at least six times. Three parallel seedlings per treatment were grown in each experiment. Samples for cytological analysis were

taken four hours after the start of light period. The concentration range used was 0.01 - 20 $\mu\text{g mL}^{-1}$ (0.01 – 20.1 μM MCY-LR).

1.2. Immunohistochemical and histochemical methods

For MT and chromatin labelling, lateral root tips were fixed with 4% (v/v) formaldehyde in phosphate buffered saline (PBS) and cryosectioned with a Leica Jung Histoslide 2000 microtome (Leica, Nussloch, Germany) to obtain 10-15 μm thick sections. Labelling of MTs with Cy3- conjugated primary anti- β -tubulin antibody (Sigma- Aldrich, St. Louis, Mo., USA) was followed by chromatin staining with 4',6'-diamidino-2-phenylindole (DAPI, Fluka, Buchs, Switzerland) as described (Beyer et al., 2012; Máthé et al., 2009). Meristematic tissues giving rise to root cortex were subjected to microscopic analysis with an Olympus AX-70 (Olympus, Tokyo, Japan) conventional fluorescence microscope (excitation wavelengths: 540-580 /Cy3/ and 320-360 nm /DAPI/) and a Zeiss LSM 510 confocal laser scanning microscope (Carl Zeiss, Jena, Germany) (excitation wavelengths: 543 /Cy3/ and 351/364 nm /DAPI/). Mitotic spindle and chromatin organization was analyzed: the types of spindle and related chromatin changes were detected and quantified. At least ten microscopic sections and 200 spindles were examined for each treatment per experiment.

For the assay of ROS levels, we used a modified 2', 7'-dichlorofluorescein-diacetate (DCFH-DA) staining method of Guo et al. (2008): whole living lateral roots were washed with PBS, incubated for 30 min in the presence of 20 μM DCFH-DA, washed twice with PBS and examined with Olympus AX-70 (Olympus, Tokyo, Japan) fluorescence microscope (excitation wavelength range: 450-480 nm). The fluorescence intensity was estimated with ImageJ64 software and quantified as area integrated optical density (AIOD). DCFH-DA is

suitable mainly for the detection of H_2O_2 and O_2^- (Caldefie-Chézet et al., 2002). At least six roots per treatment were analyzed for ROS levels in each experiment.

The percentage of spindle anomalies per total spindle number (100%) was counted and the intensities of DCFH-DA labelling were analyzed, and then the mean \pm SE values were plotted with the aid of Sigma Plot® 10.0 software, or are shown on Tables 1-2.

1.3. The assay of protein phosphatase activity

Total protein phosphatase (PP1 and PP2A) activity was measured as described previously (Máthé et al., 2009, 2013a). Whole roots were extracted with a buffer containing 50 mM Tris-HCl (pH 7.5), 0.1 mM EDTA, 0.2 mM EGTA, 0.1% (w/v) DTT and 0.2 mM PMSF (Sigma-Aldrich). Specific phosphatase activities were given as pmol [^{32}Pi] released mg protein $^{-1}$ (Erdódi et al., 1995) and presented as the percentage of control activities (100 %) by plotting with the aid of Systat Sigma Plot 10.0 ® software. The protein content of cell-free extracts was assayed by the method of Bradford (1976).

1.4. Determination of peroxidase (POD) and catalase (CAT) activities

Enzymatic antioxidant activities were detected on native 7.5% polyacrylamide gels. Crude enzyme extracts of plant tissue samples were prepared in a buffer containing 150 mM NaCl (Reanal, Budapest, Hungary), 14.6 mM 2-mercaptoethanol (Sigma-Aldrich) in 100 mM Tris-HCl (Sigma-Aldrich) pH 8.0 (Schlereth et al., 2000). Buffers were added at a 2:1 buffer:tissue FW ratio. After repeated centrifugations at 15,000 x g with a Heraeus Biofuge, 20 μL of supernatants were loaded onto the gels, therefore each sample contained 7-8 mg (FW) of plant material. For the detection of pyrogallol peroxidase bands, native gels were incubated in

50mM K_2HPO_4/KH_2PO_4 buffer, pH 7.5, then stained for 15-30 min in the same buffer containing 20 mM pyrogallol and 5 mM H_2O_2 . The oxidation product (purpurogallin) was detected as a pattern of dark brown colored bands.

For the detection of catalase isoenzymes, a standard protocol was used (see Weidert and Cullen, 2010). Gels were incubated in 0.03% H_2O_2 for 15 min, followed by a washing step. Afterwards, they were incubated in 0.76 mM $K_3[Fe(CN)_6]$ and 1.5 mM $FeCl_3$, pH 7.5, then analyzed. Catalase activities were detected as transparent bands on a dark background.

Gels were analyzed with the aid of CP Atlas® software. Total band intensities were calculated on the basis of peak areas given by the enzyme activities, then plotted with the aid of Systat Sigma Plot 10.0 ® software.

1.5. Data analysis

All experiments were repeated at least six times. The data for (sum of) altered spindles, DCFH-DA staining, total PP1/PP2A enzyme activities and CAT, POD enzyme band intensities were subjected to one-way analysis of variance (ANOVA). The means of treatments were compared against controls using Dunn's or Dunnett's post hoc tests depending on whether there were an equal or unequal number of data of groups. Levels of significance ($P < 0.05$) are indicated with asterisks, where appropriate.

2. Results

2.1. The effects of MCY-LR on metaphase and anaphase spindle organization

Control metaphases in *V. faba* lateral root meristems were characterized by normal bipolar spindle organization with normal chromosome alignment in the equatorial plane. Top view of metaphase showed that at each pole, spindle MTs originated from multiple and near evenly dispersed nucleation sites (Fig. 1a, b). Control anaphases showed normal bipolar spindles characterized by shortening of MT bundles, narrowing of spindles and normal sister chromatid segregation (Fig. 2a).

One day of treatments with MCY-LR did not induce significant changes in mitotic spindle organization. In contrast, 2 and 6 day treatments resulted in the formation of diverse types of spindle anomalies summarized in Tables 1.-2. Most of the spindle alteration types were defined according to Shamina (2005) and are presented below.

- (a) Disrupted or chaotic spindles showed partially or totally disorganized MT structures developed with high frequency at 2 and 6 day treatments with 0.1 and 5-10 $\mu\text{g mL}^{-1}$ MCY-LR in metaphase cells (Fig. 1e). At 10 $\mu\text{g mL}^{-1}$ MCY-LR (2 days' exposure) and 5 $\mu\text{g mL}^{-1}$ MCY-LR (6 days' exposure) they were detected in anaphase cells as well (Tables 1-2).
- (b) Spindles with additional polar MT bundles were characterized by excessive bundling of interpolar MT fibers and appeared in metaphase cells in the presence of 0.1 $\mu\text{g mL}^{-1}$ MCY-LR after 6 days of toxin treatment (Fig. 1f).
- (c) Tripolar/multipolar spindles were characterized by MT nucleation sites originating from more than two poles (Fig. 1c, 2b). This type of alteration was the most characteristic for 6 days of MCY-LR treatment of *V. faba* roots: it was detected at 0.5-20 $\mu\text{g mL}^{-1}$ MCY-LR in metaphase cells (highest percentage at 0.5 $\mu\text{g mL}^{-1}$ MCY-LR, Table 2) and at 1 and 10 $\mu\text{g mL}^{-1}$ MCY-LR in anaphase cells (highest percentage at 10 $\mu\text{g mL}^{-1}$ MCY-LR, Table 2). Multipolar spindles were detected in metaphase lateral

- root cells from seedlings treated for 2 days with $10 \mu\text{g mL}^{-1}$ MCY-LR as well (Table 1.).
- (d) Multipolar spindles with hyperbundled kinetochore MTs showed excessive bundling of midplane MTs arising from both poles. They were observed in metaphase cells after 6 days' treatment with $0.1 \mu\text{g mL}^{-1}$ MCY-LR (Fig. 1g).
- (e) Monopolar spindles were characteristic for metaphase cells and were characterized by MT nucleation at only one pole of dividing cell (Fig. 1h). They were detected at $1-10 \mu\text{g mL}^{-1}$ MCY-LR (2 days' exposure) and $5-20 \mu\text{g mL}^{-1}$ MCY-LR (6 days' exposure).
- (f) Incomplete spindles showed missing kinetochore fibers, revealed by top views of mitotic figures. They were associated with rosette-like arrangement of hypercondensed chromosomes in metaphase (Fig. 1d) and appeared at treatments with $10 \mu\text{g mL}^{-1}$ MCY-LR (2 days' exposure, metaphase cells) and $10-20 \mu\text{g mL}^{-1}$ MCY-LR in metaphase and $20 \mu\text{g mL}^{-1}$ MCY-LR in anaphase cells (6 days' exposure).
- (g) Distorted (bent) spindles appeared in metaphase cells. Bending was characteristic for MTs arising from both poles. They were of two types: C-shaped and S-shaped (Fig. 1i, j). Their formation was induced at $10-20 \mu\text{g mL}^{-1}$ MCY-LR (2 and 6 days' exposure).
- (h) Additional spindles (possibly variants of multipolar spindle) showed an extra microtubular structure frequently situated at the midplane of metaphase cells (Fig. 1k) induced by 6 days' exposure to 0.1 and $10 \mu\text{g mL}^{-1}$ MCY-LR.
- (i) Midplane kinetochore fibers were detected in anaphase cells and showed strongly bundled midplane MTs accompanied with the formation of lagging chromosomes (Fig. 2c). They were detected at 6-day treatments with $20 \mu\text{g mL}^{-1}$ MCY-LR.
- (j) Asymmetrical spindles were detected in metaphase characterized by unequal sizes of MT arrays arising from the two poles and detected at $10 \mu\text{g mL}^{-1}$ MCY-LR both at 2 and 6 days of toxin exposure (Fig. 1l).

Quantification of total mitotic spindle alterations revealed that control cells showed abnormal spindles in a very low percentage (2 days of toxin exposure) or did not show such anomalies at all (6 days of toxin exposure, Tables 1-2). After two days of cyanotoxin treatment, significant increases in the number of aberrant metaphase spindles were detected at $10 \mu\text{g mL}^{-1}$ MCY-LR, but no significant changes were observable in anaphase cells (Fig. 3a). In contrast, at 6 days of treatment, MCY-LR induced the formation of altered spindles in a significant and dose-dependent manner both in metaphase and anaphase cells (Fig. 3b). For metaphase, $0.01 \mu\text{g mL}^{-1}$ MCY-LR did not have any effect. Alterations appeared at treatments with $0.1 \mu\text{g mL}^{-1}$ MCY-LR and peaked at $10 \mu\text{g mL}^{-1}$ MCY-LR, where $21.15 \pm 1.47\%$ of spindles were altered (Fig. 3b, Table 2). At higher toxin concentration ($20 \mu\text{g mL}^{-1}$), the percentage of aberrant spindles decreased as compared to $10 \mu\text{g mL}^{-1}$ MCY-LR, but still remained at relatively high levels. Concerning anaphase, 0.01 - $0.5 \mu\text{g mL}^{-1}$ MCY-LR did not induce any alterations in spindle organization. In contrast, 1 - $20 \mu\text{g mL}^{-1}$ MCY-LR did induce spindle anomalies. Their highest percentage was at $5 \mu\text{g mL}^{-1}$ MCY-LR ($8.55 \pm 0.47\%$ of anaphase spindles, Fig. 3b).

We added $100 \mu\text{M}$ ascorbic acid (AsA) to culture media containing $10 \mu\text{g mL}^{-1}$ MCY-LR, followed by 2 days of plant treatment. As compared to treatments with MCY-LR only, AsA did not decrease the percentage of abnormal mitotic spindles (data not shown), i.e. an antioxidant did not protect dividing cells from the cyanotoxin-induced mitotic defects.

2.2. The effect of MCY-LR on total protein phosphatase activity of *V. faba* roots

MCY-LR had a time- and dose-dependent effect on total protein phosphatase (PP1 and PP2A) activities in *V. faba*, when measured with 20 kDa phosphorylated light chain of myosin II as substrate. $0.01 \mu\text{g mL}^{-1}$ of toxin did not have any inhibitory effect. At one day of exposure, 1 - $20 \mu\text{g mL}^{-1}$ MCY-LR decreased significantly the total PP1 and PP2A activities, but the 50%

inhibitory concentration (IC_{50}) was above $1 \mu\text{g mL}^{-1}$ MCY-LR. At 2 and 6 days of treatments (relatively long-term exposures), $0.1\text{-}20 \mu\text{g mL}^{-1}$ MCY-LR inhibited phosphatase activities significantly, IC_{50} was $0.4 \mu\text{g mL}^{-1}$ MCY-LR (Fig. 3c). At these exposures, $1\text{-}20 \mu\text{g mL}^{-1}$ MCY-LR induced severe inhibition of phosphatase activities, to $11.7 \pm 1.59\%$ of control activities (Fig. 3c).

3.3. Effects of MCY-LR on ROS levels and antioxidant enzyme activities in *V. faba* roots

Labelling of cyanotoxin-treated lateral root tips with DCFH-DA did not reveal significant changes in ROS levels. This was true for all exposure times (1, 2 and 6 days) assayed. Even though we detected a slight increase of ROS levels in root tips treated for 2 days with $1 \mu\text{g mL}^{-1}$ MCY-LR, this change was not significant (Fig. 4a).

With respect to pyrogallol peroxidase (POD) and catalase (CAT) activities, there was a time- and cyanotoxin dose dependent increase, with differences between the two enzyme systems (Fig. 4b, c). For peroxidase, $0.1 \mu\text{g mL}^{-1}$ and higher MCY-LR concentrations induced the increase of its activity with significant changes at $0.1\text{-}10 \mu\text{g mL}^{-1}$ at 1 day and $1, 10 \mu\text{g mL}^{-1}$ at 6 days of exposure, with the most prominent change at 6 days, where $10 \mu\text{g mL}^{-1}$ MCY-LR induced a more than two-fold increase. At two days of toxin exposure, increases were significant only at $10 \mu\text{g mL}^{-1}$ MCY-LR (Fig. 4b). This cyanotoxin concentration induced a dramatic increase of catalase activity at two days of toxin treatment (Fig. 4c). $10 \mu\text{g mL}^{-1}$ MCY-LR induced significant changes in catalase activity at all exposure times, and lower concentrations ($0.1\text{-}1 \mu\text{g mL}^{-1}$ MCY-LR) induced significant increases at 1 and 6 days of treatments (Fig. 4c).

3. Discussion

We detected a wide range of mitotic spindle anomalies induced by MCY-LR, a cyanobacterial toxin. No other protein phosphatase inhibitor is known to induce such a variety of MT organization changes (see Table 3). The development of altered spindle structures in *V. faba* was time- and MCY-LR dose-dependent (Fig. 3a, b). In general, at 2 days of toxin exposure, the percentage of spindle disorders was lower than for 6 days of exposure and several spindle types- additional polar MT bundles, multipolar spindles with kinetochore MT hyperbundling, additional spindles and midplane anaphase kinetochore bundles- were not detectable at this stage (compare Tables 1-2, anomalies b, d, h and i). Only disrupted spindles were detectable at lower ($0.1 \mu\text{g mL}^{-1}$) MCY-LR concentration. $1 \mu\text{g mL}^{-1}$ MCY-LR induced the formation of 2 types of spindle disorders, while $10 \mu\text{g mL}^{-1}$ MCY-LR induced 7 types (Table 1). For 6 days of exposure, at lower toxin concentrations ($0.1\text{-}5 \mu\text{g mL}^{-1}$) 1-3 types of anomalies appeared. At higher doses, the number of types of altered spindles increased: 8 types were detected at $10 \mu\text{g mL}^{-1}$ and 6 types at $20 \mu\text{g mL}^{-1}$ MCY-LR (Table 1). This implied that certain disorders- missing kinetochore fibers, C- and S- shaped spindles, midplane kinetochore fibers and asymmetrical spindles (alterations f, g, i, j, see Results) occurred only at high toxin doses that blocked near completely PP1 and PP2A activity (Table 2; Fig. 3b). Thus, for both 2 and 6 days of toxin exposure, the number of anomalous spindle types increased with the increase of cyanotoxin concentration (Tables 1-2). Additional polar MT bundles and multipolar spindles with kinetochore MT hyperbundling (alterations b, d) occurred only under long-term (6 day) treatments with low MCY-LR concentration ($0.1 \mu\text{g mL}^{-1}$) that inhibited protein phosphatase activity by 22%. The formation of disrupted and multipolar spindles (alterations a, c) was induced by a wide range of toxin concentration (Table 2). Overall, spindle disorders occurred at MCY-LR concentrations of $0.1\text{-}20 \mu\text{g mL}^{-1}$

that significantly inhibited PP1 and PP2A activity at 2 and 6 days of toxin treatments (Fig. 3). Lower toxin dose ($0.01 \mu\text{g mL}^{-1}$ MCY-LR) neither induced the formation of altered spindles, nor inhibited protein phosphatase activity (Table 2, Fig. 3c).

The above findings suggest a relationship between the inhibition of PP1 and PP2A activities and a wide range of alterations in mitotic spindle development. However, one day of toxin treatment did not induce spindle disorganization, even though at this stage $1 \mu\text{g mL}^{-1}$ and higher MCY-LR concentrations significantly inhibited PP1 and PP2A activities (Fig. 3c). Moreover, short-term (maximum 24 h) toxin treatments are known to induce other mitotic changes- histone H3 hyperphosphorylation and consequent chromosome hypercondensation- in *V. faba* (Beyer et al., 2012). Thus, it appears that only long-term protein phosphatase inhibition is effective for MT changes. Meanwhile, it is known that MCY-LR induces oxidative stress, another mechanism that is potentially causing MT disruption in animal cells (Ding et al., 2001; Jiang et al., 2013). ROS induction is known to induce the formation of multipolar spindles and mitotic MT destabilization (Wang et al., 2013). Therefore, we were looking for a possible relationship between MCY-LR induced oxidative stress and mitotic MT disorders in *V. faba*.

DCFH-DA staining did not reveal significant increases in the ROS levels of *V. faba* lateral root tips, irrespective of the time of MCY-LR exposure and the concentration of toxin (Fig. 4a). Meanwhile, there were significant increases in the activities of the H_2O_2 scavenging enzymes POD and CAT (Fig. 4b, c). These results show that the model plant used –*V. faba*- is able of efficient defense against oxidative stress. Indeed, there is evidence that at least some cultivars of broad bean are producing secondary metabolites –e.g. phenolics and the alkaloids vicine, divicine – capable of efficient ROS scavenging (El-Maksoud et al., 2013; Shetty et al., 2002). Meanwhile, MCY-LR does induce oxidative stress in animals and plants (including aquatic plants) more susceptible to ROS accumulation (Campos and Vasconcelos, 2010;

Pflugmacher, 2002). The *V. faba* cultivar used in this study seems to be resistant to oxidative stress. Therefore, the induction of MT disorders by elevated ROS caused by MCY-LR can be excluded in this system. *Vicia* could be an excellent model for the study of cytological consequences of MCY-LR-induced protein phosphatase inhibition as taken apart from the ROS-inducing activity of toxin.

Taken together, all of these findings strongly suggest that indeed, long-term protein phosphatase inhibition is the primary cause of mitotic MT disorders in *V. faba*. The main arguments in favor of this statement are: (i) Under 2 day treatments, most MT disorders occur at $10 \mu\text{g mL}^{-1}$ MCY-LR that induced near total inhibition of PP1 and PP2A. One day of MCY-LR exposure does not induce notable spindle disorders even at $10 \mu\text{g mL}^{-1}$, where strong phosphatase inhibition occurs; (ii) there is no significant increase of ROS in MCY-LR treated root tips; (iii) ascorbic acid (AsA) is known for a long time to be a strong antioxidant and as such, it can prevent plant cells from oxidative stress induced by ROS (Thompson et al., 1987). Moreover, AsA deficiency induces increased sensitivity of model plants to oxidative stress (Conklin et al., 1996). Exogenously applied AsA can have beneficial effects on cell cycle progression (Conklin, 2001). When L-galactono- γ -lactone, the precursor of AsA was applied to tobacco BY-2 cells, a mitotic peak was observed, while dehydro-ascorbic acid had inhibitory effects on mitosis (de Pinto et al., 1999). In spite of all these previous observations, in our experiments AsA could not protect meristematic cells from MCY-LR-induced MT disorders. Thus, it is likely that MCY-LR does not affect spindle architecture via ROS induction in *V. faba*.; (iv) 6 days of MCY-LR exposure induces more types and higher frequency of spindle disorders, than 2 days of exposure; (v) a wide variety of protein phosphatase inhibitors are able to induce spindle organization anomalies (Table 3).

Table 3 summarizes all types of mitotic spindle alterations induced by protein phosphatase inhibitors. Disrupted, multipolar and distorted spindles (alterations a, c and g)

were induced by several toxins in a wide range of eukaryotic organisms. However, MCY-LR induces a much wider range of spindle anomalies than any other inhibitors. Except calyculin A, drugs other than MCY-LR involved in these studies are known to inhibit primarily PP2A, with less potency for PP1. However, the inhibition of PP1 activity/ expression is known to alter spindle architecture as well. Multipolar spindles were detected in neuroblast cells of a *Drosophila* mutant deficient in a PP1 isoenzyme. The authors correlated this to abnormal centrosome replication (Axton et al., 1990). The above findings show that both PP1 and PP2A play a role in normal spindle polarity. To the best of our knowledge, the present study is the first one showing the formation of additional polar MT bundles, multipolar spindles with kinetochore MT hyperbundling, incomplete, additional spindles and midplane kinetochore fiber bundles (alterations b, d, f, h, i) induced by a protein phosphatase inhibitor (Table 3). Overall, MCY-LR seems to induce a higher variety of spindle disorders than any other protein phosphatase inhibitor that might be related to its complex effects on protein phosphatases. It inhibits PP1, PP2A as well as PP4, PP5 (phosphatases also involved in mitotic regulation) with similar potency (Cohen et al., 2005; MacKintosh and Diplexcito, 2003).

What are the possible cellular/molecular mechanisms of long-term protein phosphatase inhibition induced spindle disorders in MCY-LR treated *V. faba*? As in all eukaryotic cells, plant microtubule associated proteins (MAPs) play important regulatory roles in MT nucleation, stability, bundling and orientation (see Hamada, 2007 for a review). It has long been known that hyperphosphorylation of MAPs alters MT organization in eukaryotic cells (Komis et al., 2011; Maccioni and Cambiazo, 1995). This is true for non-mitotic and mitotic plant cells as well. When proteins belonging to the MAP65 family are hyperphosphorylated, MT binding and consequent MT bundling and organization is impaired during mitosis (Sasabe et al., 2006; Smertenko et al., 2006). Therefore, we propose that MCY-LR, as a protein phosphatase inhibitor, can influence the phosphorylation state of MAPs involved in

mitotic spindle organization, inducing a significant number of spindle anomalies as shown for *V. faba* root tip meristems. In addition, protein phosphatase inhibition is known to alter spindle polarity in all eukaryotic cells. In animal cells, it will inhibit centrosome replication at the beginning of mitosis (Axton et al., 1990; Schlaitz et al., 2007). One may assume that in plant cells characterized by anastral mitosis, it will prevent the proper functioning of MTOCs involved in the establishment of normal spindle polarity. Therefore, the formation of monopolar and multipolar spindles (alterations c, e) induced by MCY-LR may be attributed to alterations of both MAP and MTOC functioning.

What is the consequence of abnormal spindle architecture? Spindle disorganization implies that sister chromatid segregation will not occur properly (Kline-Smith and Walczak, 2004). We have previously detected that MCY-LR delays metaphase-anaphase transition and monopolar/ multipolar spindles induce the formation of lagging chromosomes (Beyer et al., 2012). Recent models of mitotic spindle architecture show that both k-fibers (kinetochore MTs) and interpolar MT bundles (polar fibers) show extensive branching that contributes to spindle stabilization (Ambrose and Cyr, 2008). Therefore, additional polar MT bundles and the hyperbundling of kinetochore MTs in metaphase and anaphase cells in the presence of MCY-LR (alterations b, d, i) might influence spindle stability, and hence alter mitotic division. Indeed, anaphase midplane bundles were accompanied by lagging chromosomes (Fig. 2c). In addition, monopolar and incomplete spindles (alterations e, f, the latter characterized by missing kinetochore fibers) were frequently accompanied by the formation of metaphase chromosome rosettes, where centromeres are oriented centrally and chromosome arms are oriented towards the periphery of MCY-LR treated *V. faba* cells (Fig. 1d). Chromosome rosettes are frequently correlated with chromosome hypercondensation and chromatid mis-segregation (Beyer et al., 2012; Nagele et al., 1998).

In conclusion, MCY-LR induced time-and dose- dependent formation of a surprisingly high number of types of spindle assembly disorders in meristematic cells of *V. faba*. Moreover, this toxin induces a far more variety of mitotic MT anomalies, than any other known protein phosphatase inhibitor (Table 3). We can state that all types of spindle anomalies detected in this study were related to the long-term PP1 and PP2A inhibitory effects of MCY-LR, since significant protein phosphatase inhibition, but no ROS induction was detected. Thus, *V. faba* is a good model to study the relationship between MCY-LR induced protein phosphatase inhibition and mitotic MT disorder, because the ROS inducing effect of the cyanotoxin is disabled in this system. To the best of our knowledge, this is the first report showing that MCY-LR induces the formation of additional polar MT bundles, excessive bundling of midplane MTs, incomplete, C-, S- shaped and additional spindles- the first three anomalies are the first detected for any protein phosphatase inhibitor. We show that MCY-LR could be a powerful tool in the understanding of the regulation of mitotic spindle organization. Our results provide new insights into the role of protein phosphatases in this subcellular event in plants and generally, in eukaryotic cells.

Acknowledgements

This research was supported by the Hungarian National Research Foundation Grants OTKA K81371 and K109249, the TÁMOP-4.2.2/A-11/1/KONV-2012-0025 project and the “Diószegi Summer School 2013” Programme (NTP-FTNYT-MPA-12-027). T. Garda, Z. Kónya, and M. Riba were supported by The Eötvös Loránd Student Fellowship Program - TÁMOP4.2.4.A/2-11-1-2012-0001 „National Excellence Program – Elaborating and operating an inland student and researcher personal support system.” The project was subsidized by the European Union and co-financed by the European Social Fund. We

acknowledge Dr. Tibor Szerdahelyi (Szent István University, Gödöllő, Hungary) and Zoltán Molnár (University of West Hungary, Mosonmagyaróvár) for seeds of *V. faba* and Mórió Miczi for his help in microscopic techniques.

Conflict of interest

The authors declare that there are no conflicts of interest.

References

- Ambrose, J.C., Cyr, R., 2008. Mitotic spindle assembly and function, in: Verma, D.P.S., Hong, Z. (Eds.), *Cell division control in plants*, Plant Cell Monographs, Springer, Berlin-Heidelberg, pp. 141-167.
- Axton, J.M., Dombrádi, V., Cohen, P.T.W., Glover, D.M., 1990. One of the protein phosphatase 1 isoenzymes in *Drosophila* is essential for mitosis. *Cell* 63, 33-46.
- Ayaydin, F., Vissi, E., Mészáros, T., Miskolczi, P., Kovács, I., Fehér, A., Dombrádi, V., Erdődi, F., Gergely, P., Dudits, D., 2000. Inhibition of serine/threonine-specific protein phosphatases causes premature activation of cdc2MsF kinase at G2/M transition and early microtubule organisation in alfalfa. *Plant J.* 23, 85-96.
- Babica, P., Bláha, L., Maršálek, B., 2006. Exploring the natural role of microcystins- a review of effects on photoautotrophic organisms. *J. Phycol.* 42, 9-20.
- Baskin, T.I., 2000. The cytoskeleton, in: Buchanan, B., Gruissem, W., Jones, R. (Eds.), *Biochemistry and molecular biology of plants*, ASPB, Rockville, Maryland, pp. 202-258.
- Beyer, D., Tándor, I., Kónya, Z., Bátor, R., Roszik, J., Vereb, G., Erdődi, F., Vasas, G., M-Hamvas, M., Jambrovics, K., Máthé, C., 2012. Microcystin-LR, a protein phosphatase

- inhibitor induces alterations in mitotic chromatin and microtubule organization leading to the formation of micronuclei in *Vicia faba*. *Ann. Bot.* 110, 797-808.
- Bollen, M., Gerlich, D.W., Lesage, B., 2009. Mitotic phosphatases: from entry guards to exit guides. *Trends Cell Biol.* 19, 531-541.
- Bonness, K., Aragon, I.V., Rutland, B., Ofori-Acquah, S., Dean, N.M., Honkanen, R.E., 2006. Cantharidin-induced mitotic arrest is associated with the formation of aberrant mitotic spindles and lagging chromosomes resulting, in part, from the suppression of PP2A α . *Mol. Cancer Ther.* 5, 2727-2736.
- Bradford, M.M., 1976. A rapid and sensitive method for the quantitation of microgram quantities of protein utilizing the principle of protein-dye binding. *Anal. Biochem.* 72, 248-254.
- Caldefie-Chézet, F., Walrand, S., Moinard, C., Tridon, A., Chassangne, J., Vasson, M.P., 2002. Is the neutrophil reactive oxygen species measured by luminol and lucigenin chemoluminescence intra or extracellular? Comparison with DCFH-DA flow cytometry and cytochrome c reduction. *Clin. Chim. Acta* 319, 9-17.
- Campos, A., Vasconcelos, V., 2010. Molecular mechanisms of microcystin toxicity in animal cells. *Int. J. Mol. Sci.*, 11, 268-287.
- Carmichael, W.W., 1992. Cyanobacteria secondary metabolites—the cyanotoxins. *Journal of applied bacteriology* 72.6 : 445-459.
- Chen, J., Zang, H.Q., Shi, Z.Q., 2013. Accumulation and phytotoxicity of microcystins in vascular plants, in: Ferrão-Filho, A.S. (Ed.), *Cyanobacteria- ecology, toxicology, and management*, Nova, New York, pp. 139-151.
- Cheng, A., Balczon, R., Zuo, Z., Koons, J.S., Walsh, A.H., Honkanen, R.E., 1998. Fostriecin-mediated G2-M- phase growth arrest correlates with abnormal centrosome replication, the

- formation of aberrant mitotic spindles, and the inhibition of serine/ threonine protein phosphatase activity. *Cancer Res.* 58, 3611-3619.
- Codd, G.A., Morrison, L.F., Metcalf, J.S., 2005. Cyanobacterial toxins: risk management for health protection. *Toxicol. Appl. Pharmacol.* 203, 264-272.
- Cohen, P.T.W., Philp, A., Vázquez-Martin, C., 2005. Protein phosphatase 4 – from obscurity to vital functions. *FEBS Lett.* 579, 3278-3286.
- Conklin, P.L., Williams, E.H., Last, R.L., 1996. Environmental stress sensitivity of an ascorbic acid-deficient *Arabidopsis* mutant. *Proc. Natl. Acad. Sci. USA* 93, 9970-9974.
- Conklin, P.L., 2001. Recent advances in the role and biosynthesis of ascorbic acid in plants. *Plant Cell Environ.* 24, 383-394.
- Corbel, S., Mougin, C., Bouaïcha, N., 2014. Cyanobacterial toxins: modes of actions, fate in aquatic and soil ecosystems, phytotoxicity and bioaccumulation in agricultural crops. *Chemosphere* 96, 1-15.
- De Pinto, M.C., Francis, D., De Gara, L., 1999. The redox state of the ascorbate-dehydroascorbate pair as a specific sensor of cell division in tobacco BY-2 cells. *Protoplasma* 209, 90-97.
- Ding, W.X., Shen, H.M., Ong, C.N., 2001. Critical role of reactive oxygen species formation in microcystin-induced cytoskeleton disruption in primary cultured hepatocytes. *J. Toxicol. Env: Health A* 64, 507-519.
- El-Maksoud, H.A., Hussein, M.A., Kassem, A., 2013. Antioxidant activity of *Vicia faba* L. vicine and its o- deglycosylation product divicine. *Int. J. Pharma.* 3, 316-323.
- Erdödi, F., Tóth, B., Hirano, K., Hirano, M., Hartshorne, D.J., Gergely, P., 1995. Endothall thioanhydride inhibits protein phosphatases-1 and -2A in vivo. *Am. J. Physiol.* 269, C1176-C1184.

- Gamborg, O.L., Miller, R.A., Ojima, K., 1968. Nutrient requirements of suspension cultures of soybean root cells. *Exp. Cell Res.* 50, 151-158.
- Guo, K., Xia, K., Yang, Z.M., 2008. Regulation of tomato lateral root development by carbon monoxide and involvement in auxin and nitric oxide. *J. Exp. Bot.* 59, 3443–3452.
- Hamada, T., 2007. Microtubule associated proteins in higher plants. *J. Plant Res.* 120, 79-98.
- Jiang, J., Gu, X., Song, R., Wang, X., Yang, L., 2011. Microcystin-LR induced oxidative stress and ultrastructural alterations in mesophyll cells of submerged macrophyte *Vallisneria natans* (Lour.) Hara. *J. Hazard. Mater.* 190, 188-196.
- Kline-Smith, S.L., Walczak, C.E., 2004. Mitotic spindle assembly and chromosome segregation: refocusing on microtubule dynamic. *Mol. Cell* 15, 317-327.
- Komis, G., Illés, P., Beck, M., Šamaj, J., 2011. Microtubules and mitogen-activated protein kinase signalling. *Curr. Op. Plant Biol.* 14, 650-657.
- Kós, P., Gorzó, G., Surányi, G., Borbely, G., 1995. Simple and efficient method for isolation and measurement of cyanobacterial hepatotoxins by plant tests (*Sinapis alba* L.). *Anal. Biochem.* 225, 49-53.
- Lankoff, A., Banasik, A., Obe, G., Deperas, M., Kuzminski, K., Tarczyska, M., Jurczak, T., Wojcik, A., 2003. Effect of microcystin-LR and cyanobacterial extract from Polish reservoir of drinking water on cell cycle progression, mitotic spindle, and apoptosis in CHO-K1 cells. *Toxicol. Appl. Pharmacol.* 189, 204-213.
- Luan, S., 2003. Protein phosphatases in plants. *Annu. Rev. Plant Biol.* 54, 63-92.
- Maccioni, R.B., Cambiazo, V., 1995. Role of microtubule-associated proteins in the control of microtubule assembly. *Physiol. Rev.* 75, 835-864.
- MacKintosh, C., Diplexcito, J., 2003. Naturally occurring inhibitors of serine/threonine phosphatases, in: Wells, J., Hunter, T., Karin, M., Farquhar, M., Thompson, B. (Eds.), *Handbook of cell signaling*. Vol.1., Elsevier., USA, pp. 607-611.

- Manzanero, S., Rutten, T., Kotseruba, V., Houben, A., 2002. Alterations in the distribution of histone H3 phosphorylation in mitotic plant chromosomes in response to cold treatment and the protein phosphatase inhibitor cantharidin. *Chromosome Res.* 10, 467-476.
- Máthé, C., Beyer, D., Erdődi, F., Serfőző, Z., Székvölgyi, L., Vasas, G., M-Hamvas, M., Jámbrik, K., Gonda, S., Kiss, A., Szigeti, Z.M., Surányi, G., 2009. Microcystin-LR induces abnormal root development by altering its microtubule organization in tissue-cultured common reed (*Phragmites australis*) plantlets. *Aquat. Toxicol.* 92, 122-130.
- Máthé, C., Vasas, G., Borbély, G., Erdődi, F., Beyer, D., Kiss, A., Surányi, G., Gonda, S., Jámbrik, K., M-Hamvas, M., 2013a. Histological, cytological and biochemical alterations induced by microcystin-LR and cylindrospermopsin in white mustard (*Sinapis alba* L.) seedlings. *Acta Biol. Hung.* 64, 75-89.
- Máthé, C., M-Hamvas, M., Vasas, G., 2013b. Microcystin-LR and cylindrospermopsin induced alterations in chromatin organization of plant cells. *Mar. Drugs* 11, 3689-3717.
- Máthé, C., Vasas, G., Surányi, G., Bácsi, I., Beyer, D., Tóth, S., Timár, M., Borbély, G., 2007. Microcystin-LR, a cyanobacterial toxin, induces growth inhibition and histological alterations in common reed (*Phragmites australis*) plants regenerated from embryogenic calli. *New Phytol.*, 176, 824-835.
- Murashige, T., Skoog, F., 1962. A revised medium for rapid growth and bioassays with tobacco tissue cultures. *Physiol. Plantarum*, 15, 473-497.
- Nagele, R.G., Freeman, T., Fazekas, J., Lee, K.-M., Thomson, Z., Lee, H.Y., 1998. Chromosome spatial order in human cells: evidence for early origin and faithful propagation. *Chromosoma* 107, 330-338.
- Olszewska, M.J., Marciniak, K., Kuran, H., 1990. The timing of synthesis of proteins required for mitotic spindle and phragmoplast in partially synchronized root meristems of *Vicia faba* L.. *Eur. J. Cell Biol.* 53, 89-92.

- Pflugmacher, S., 2002. Possible allelopathic effects of cyanotoxins, with reference to microcystin-LR, in aquatic ecosystems. *Environ. Toxicol.* 17, 407–413.
- Roberge, M., Tudan, C., Hung, S.M.F., Harder, K.W., Jirik, F.R., Anderson, H., 1994. Antitumor drug fostriecin inhibits the mitotic entry checkpoint and protein phosphatases 1 and 2A. *Cancer Res.* 54, 6115-6121.
- Sakurada, K., Zheng, B., Kuo, J.F., 1992. Comparative effects of protein phosphatase inhibitors (okadaic acid and calyculin A) on human leukemia HL60, HL60/ADR and K562 cells. *Biochem. Biophys. Res. Commun.* 187, 488-492.
- Sasabe, M., Soyano, T., Takahashi, Y., Sonobe, S., Igarashi, H., Itoh, T.J., Hidaka, M., Machida, Y., 2006. Phosphorylation of NtMAP65-1 by a MAP kinase down-regulates its activity of microtubule bundling and stimulates progression of cytokinesis of tobacco cells. *Gene Dev.* 20, 1004-1014.
- Schlaitz, A.L., Srayko, M., Dammermann, A., Quintin, S., Wielsch, N., MacLeod, I., De Robillard, Q., Zinke, A., Müller-Reichert, T., Shevchenko, A., Oegema, K., Hyman, A.A., 2007. The *C. elegans* RSA complex localizes protein phosphatase 2A to centrosomes and regulates mitotic spindle assembly. *Cell* 128, 115-127.
- Schlereth, A., Becker, C., Horstmann, C., Tiedemann, J., Müntz, K., 2000. Comparison of globulin mobilization and cysteine proteinases in embryogenic axes and cotyledons during germination and seedling growth of vetch (*Vicia sativa* L.). *J Exp. Bot.* 51, 1423–1433.
- Shamina, N.V., 2005. A catalogue of abnormalities in the division spindles of higher plants. *Cell Biol. Int.* 29, 384-391.
- Shetty, P., Atallah, M.T., Shetty, K., 2002. Effects of UV treatment on the proline-linked pentose phosphate pathway for phenolics and L-DOPA synthesis in dark germinated *Vicia faba*. *Process Biochem.* 37, 1285-1295.

- Smertenko, A.P., Chang, H.-Y., Sonobe, S., Fenyk, S.I., Weingartner, M., Bögre, L., Hussey, P.J., 2006. Control of the AtMAP65-1 interaction with microtubules through the cell cycle. *J. Cell Sci.* 119, 3227-3237.
- Thompson, J.E., Legge, R.L., Barber, R.F., 1987. The role of free radicals in senescence and wounding. *New Phytol.* 105, 317-344.
- Toivola, D.M., Eriksson, J.E., 1999. Toxins affecting cell signalling and alteration of cytoskeletal structure. *Toxicol. in Vitro* 13, 521-530.
- Van Dolah, F.M., Ramsdell, J.S., 1992. Okadaic acid inhibits a protein phosphatase activity involved in formation of the mitotic spindle of rat GH₄ rat pituitary cells. *J. Cell. Physiol.* 152, 190-198.
- Vandré, D.D., Wills, V.L., 1992. Inhibition of mitosis by okadaic acid: possible involvement of a protein phosphatase 2A in the transition from metaphase to anaphase. *J. Cell. Sci.* 101, 79-91.
- Vasas, G., Gáspár, A., Páger, C., Surányi, G., Máthé, C., M-Hamvas, M., Borbély, G., 2004. Analysis of cyanobacterial toxins (anatoxin-a, cylindrospermopsin, microcystin-LR) by capillary electrophoresis. *Electrophoresis* 25, 108-115.
- Wang, C.Y., Liu, L.N., Zhao, Z.B., 2013. The role of ROS toxicity in spontaneous aneuploidy in cultured cells. *Tissue Cell* 45, 47-53.
- Weidert, C.J., Cullen, J.J., 2010. Measurement of superoxide dismutase, catalase and glutathione peroxidase in cultured cells and tissue. *Nat. Protoc.* 5, 51-66.
- Žegura, B., Štraser, A., Filipič, M., 2011. Genotoxicity and potential carcinogenicity of cyanobacterial toxins- a review. *Mutat. Res. -Rev. Mutat.* 727, 16-41.

Figure captions

Fig. 1. The effects of microcystin-LR (MCY-LR) on the formation of aberrant metaphase spindles in *V. faba* lateral root meristems (image **k** is of a cell in metaphase-early anaphase). Images (**a-d**) show anti- β -tubulin labelling of microtubules (MTs) (cy3), histochemical staining of chromatin with DAPI and merged image of the two labelling procedures (m). Images (**e-l**) are showing anti- β -tubulin labelling. (**a**) control metaphase, side view; (**b**) control metaphase, top view; (**c**) side view of a developing tripolar spindle (cell treated with $10 \mu\text{g mL}^{-1}$ MCY-LR); (**d**) top view of an incomplete spindle and rosette-like arrangement of chromosomes (cell treated with $20 \mu\text{g mL}^{-1}$ MCY-LR); (**e**) disrupted spindle (cell treated with $10 \mu\text{g mL}^{-1}$ MCY-LR); (**f**) spindle with additional polar MT bundle (arrow) (cell treated with $0.1 \mu\text{g mL}^{-1}$ MCY-LR); (**g**) multipolar spindle with hyperbundling of kinetochore MT fibers (arrowheads) (cell treated with $0.1 \mu\text{g mL}^{-1}$ MCY-LR); (**h**) monopolar spindle (cell treated with $10 \mu\text{g mL}^{-1}$ MCY-LR) (**i**) C-shaped spindle (cell treated with $20 \mu\text{g mL}^{-1}$ MCY-LR); (**j**) S-shaped spindle (cell treated with $10 \mu\text{g mL}^{-1}$ MCY-LR); (**k**) additional spindle (arrow) (cell treated with $10 \mu\text{g mL}^{-1}$ MCY-LR); (**l**) asymmetrical spindle (cell treated with $10 \mu\text{g mL}^{-1}$ MCY-LR). Conventional fluorescence (a-d, f, g, i, l) and confocal microscopy (e, h, j, k) images. Scalebars: $5 \mu\text{m}$. Chromatin labelling of cells of (e-l) is shown on Supplementary Fig. 1.

Fig. 2. The effects of microcystin-LR (MCY-LR) on the formation of aberrant anaphase spindles in *V. faba* lateral root meristems. Images show anti- β -tubulin labelling of microtubules (MTs) (cy3), histochemical staining of chromatin with DAPI and merged image of the two labelling procedures (m). (**a**) control anaphase; (**b**) tripolar anaphase spindle (cell treated with $1 \mu\text{g mL}^{-1}$ MCY-LR); (**c**) midplane kinetochore fibers (arrow) and a lagging

chromosome (arrowhead) (cell treated with $20 \mu\text{g mL}^{-1}$ MCY-LR). Conventional fluorescence (c) and confocal microscopy (a, b) images. Scalebars: $5 \mu\text{m}$.

Fig. 3. Dose- dependent effects of MCY-LR on the formation of aberrant spindles in lateral root tip meristematic cells: 2 days (**a**) and 6 days (**b**) treatments. Time-and dose dependent effects on total protein phosphatase (PP1 and PP2A) activity of roots (**c**). *statistically significant differences, $P < 0.05$.

Fig. 4. The time- and dose-dependent effects of MCY-LR on ROS levels and oxidative stress defence enzyme activities. (**a**) Effects on ROS levels as revealed by DCFH-DA staining of lateral root tips. Representative microscopic images of DCFH-DA labelling are shown on Supplementary Fig. 2; (**b**) changes in pyrogallol peroxidase activities, the upper panel shows a characteristic native activity gel; (**c**) changes in catalase activities, the upper panel shows a characteristic native activity gel. *statistically significant differences, $P < 0.05$.

Table 1 Percentage of spindle anomalies out of total metaphase/ anaphase spindles induced by 2 days' treatment with MCY-LR in *V. faba* lateral root meristems. Mean \pm SE values are presented.

Type of spindle alteration	MCY-LR, $\mu\text{g ml}^{-1}$			
	0	0.1	1	10
a. disrupted spindle				
metaphase	0.48 \pm 0.15	1.11 \pm 0.33	0.62 \pm 0.23	2.63 \pm 0.57
anaphase	0	0	0	0.79 \pm 0.2
c. tripolar/ multipolar spindle				
metaphase	0	0	0	0.7 \pm 0.28
anaphase	0	0	0	0
e. monopolar spindle				
metaphase	0	0	0.41 \pm 0.11	4.73 \pm 1.3
anaphase	0	0	0	0
f. incomplete spindle (missing kinetochore fibers)				
metaphase	0	0	0	1.01 \pm 0.29
anaphase	0	0	0	0
g1. C-shaped spindle				
metaphase	0	0	0	0.92 \pm 0.33
anaphase	0	0	0	0
g2. S-shaped spindle				
metaphase	0	0	0	0.3 \pm 0.15
anaphase	0	0	0	0
j. asymmetrical (unequal) spindle				
metaphase	0	0	0	0.95 \pm 0.26
anaphase	0	0	0	0
Sum of total spindle anomalies				
metaphase	0.48 \pm 0.15	1.11 \pm 0.33	1.00 \pm 0.27	11.72 \pm 1.8
anaphase	0	0	0	0.79 \pm 0.2

Table 2 Percentage of spindle anomalies out of total metaphase/ anaphase spindles induced by 6 days' treatment with MCY-LR in *V. faba* lateral root meristems. Mean \pm SE values are presented.

Type of spindle alteration	MCY-LR, $\mu\text{g ml}^{-1}$							
	0	0.01	0.1	0.5	1	5	10	20
a. disrupted spindle								
metaphase	0	0	4.92 \pm 0.42	0	0	4.16 \pm 0.31	3.02 \pm 0.29	0
anaphase	0	0	0	0	0	8.54 \pm 0.58	0	0
b. additional polar MT bundles								
metaphase								
anaphase	0	0	1.23 \pm 0.05	0	0	0	0	0
	0	0	0	0	0	0	0	0
c. tripolar/ multipolar spindle								
metaphase	0	0	0	10.12 \pm 0.59 ⁱ	9.37 \pm 0.44 ⁱ	4.16 \pm 0.5 ⁱ	3.02 \pm 0.16 ⁱ	1.53 \pm 0.13 ⁱ
anaphase	0	0	0	0	5.55 \pm 0.45 ⁱ	0	5.88 \pm 0.85 ⁱ	0
d. multipolar spindle with hyperbundling of kinetochore MTs								
metaphase								
anaphase	0	0	1.23 \pm 0.09	0	0	0	0	0
	0	0	0	0	0	0	0	0

e. monopolar spindle

metaphase	0	0	0	0	0	4.16 ± 0.3^i	3.02 ± 0.36^i	1.53 ± 0.09^i
anaphase	0	0	0	0	0	0	0	0

f. incomplete spindle

(missing kinetochore fibers)

metaphase

anaphase	0	0	0	0	0	0	1.51 ± 0.15	1.53 ± 0.13
	0	0	0	0	0	0	0	1.47 ± 0.17

g1. C-shaped spindle

metaphase	0	0	0	0	0	0	1.51 ± 0.13	3.07 ± 0.29
anaphase	0	0	0	0	0	0	0	0

g2. S-shaped spindle

metaphase	0	0	0	0	0	0	3.02 ± 0.36	0.77 ± 0.05
anaphase	0	0	0	0	0	0	0	0

h. additional spindle

metaphase	0	0	1.23 ± 0.12	0	0	0	4.54 ± 0.28	0
anaphase	0	0	0	0	0	0	0	0

i. midplane**kinetochore fiber****bundles**

metaphase

anaphase	0	0	0	0	0	0	0	0
	0	0	0	0	0	0	0	1.47 ± 0.13^i

j. asymmetrical**(unequal) spindle**

metaphase

anaphase	0	0	0	0	0	0	1.51 ± 0.11	0
	0	0	0	0	0	0	0	0

Sum of total spindle**anomalies**

metaphase	0	0	8.64 ± 0.23	10.12 ± 0.59	9.37 ± 0.44	12.48 ± 1.0	± 1.47	8.35 ± 0.9
anaphase	0	0	0	0	5.55 ± 0.45	8.54 ± 0.58	5.88 ± 0.85	2.94 ± 0.29

ⁱspindle anomalies accompanied with abnormal mitotic chromatin organization/ sister chromatid segregation as detected by histochemical analysis

Table 3 Types of mitotic spindle anomalies induced by PP1 and/ or PP2A inhibitors

Type of spindle alteration	PP1/PP2A inhibitor	Organism/ cell type where detected	Mitotic phase involved	References
a. disrupted spindle	cantharidin ^a , fostriecin ^a , MCY-LR ^b ,	Phragmites australis, V. faba roots, A549 (human) cells, BHK-21 (mammalian) cells	metaphase, anaphase	Beyer et al., 2012; Bonness et al., 2006; Cheng et al., 1998; Manzanero et al., 2002; Máthé et al., 2009; Roberge et al., 1994; this study
b. additional polar MT bundles^c	MCY-LR ^b	V. faba roots	Metaphase	this study
c. tripolar/ multipolar spindle	cantharidin ^a , calyculin A ^b , endothall ^a , fostriecin ^a , OA ^a , MCY-LR ^b	P. australis, V.faba roots, alfalfa cell suspensions, CHO K1 cells, A549 (human) cells, human leukemia cells, LLC-PK (mammalian) cells, GH ₄ (mammalian) cells	prometaphase, metaphase, anaphase	Ayaydin et al., 2000; Beyer et al., 2012; Bonness et al., 2006; Cheng et al., 1998; Lankoff et al., 2003; Máthé et al., 2009; Sakurada et al., 1992; Van Dolah and Ramsdell, 1992; Vandré and Wills, 1992; this study
d. multipolar spindle with	MCY-LR ^b	V. faba roots	Metaphase	this study

hyperbundling of kinetochore MTs^c				
e. monopolar spindle	MCY-LR ^b	V. faba roots, CHO K1 cells	Metaphase	Beyer et al., 2012; Lankoff et al., 2003; this study
f. incomplete spindle (missing kinetochore fibers)	MCY-LR ^b	V. faba roots	metaphase, anaphase	this study
g. distorted (C-or S-shaped spindle)^c	OA ^a , MCY-LR ^b	V. faba roots, LLC-PK (mammalian) cells	Metaphase	Vandré and Wills, 1992; this study
h. additional spindle^c	MCY-LR ^b	V. faba roots	Metaphase	this study
i. midplane kinetochore fiber bundles^c	MCY-LR ^b	V. faba roots	Metaphase	this study
j. asymmetrical (unequal) spindle	MCY-LR ^b	P. australis, V.faba roots	metaphase, anaphase	Máthé et al., 2009; this study
k. unstable spindle	calyculin A ^b	Caenorhabditis elegans	not defined	Schlaitz et al., 2007

^ainhibits preferentially PP2A; ^binhibits PP1 and PP2A with equal potency; ^cto the best of our knowledge, for MCY-LR, detected only in this study

